

Universal Velocity Statistics in Decaying Turbulence

Christian Küchler^{*}

Max Planck Institute for Dynamics and Self-Organization, Göttingen, Germany;
 Institute for Dynamics of Complex Systems, University of Göttingen, Göttingen, Germany;
 and Max Planck University of Twente Center for Complex Fluid Dynamics, Göttingen, Germany and Twente, Netherlands

Gregory P. Bewley[†]

Sibley School of Mechanical and Aerospace Engineering, Cornell University, Ithaca, New York, USA

Eberhard Bodenschatz[‡]

Max Planck Institute for Dynamics and Self-Organization, Göttingen, Germany;
 Institute for Dynamics of Complex Systems, University of Göttingen, 37075 Göttingen, Germany;
 Physics Department and Sibley School of Mechanical and Aerospace Engineering, Cornell University, Ithaca, 14853 New York, USA;
 and Max Planck University of Twente Center for Complex Fluid Dynamics, Göttingen, Germany and Twente 7522NB, Netherlands

 (Received 26 January 2023; revised 10 April 2023; accepted 10 May 2023; published 10 July 2023)

In turbulent flows, kinetic energy is transferred from large spatial scales to small ones, where it is converted to heat by viscosity. For strong turbulence, i.e., high Reynolds numbers, Kolmogorov conjectured in 1941 that this energy transfer is dominated by inertial forces at intermediate spatial scales. Since Kolmogorov's conjecture, the velocity difference statistics in this so-called inertial range have been expected to follow universal power laws for which theoretical predictions have been refined over the years. Here we present experimental results over an unprecedented range of Reynolds numbers in a well-controlled wind tunnel flow produced in the Max Planck Variable Density Turbulence Tunnel. We find that the measured second-order velocity difference statistics become independent of the Reynolds number, suggesting a universal behavior of decaying turbulence. However, we do not observe power laws even at the highest Reynolds number, i.e., at turbulence levels otherwise only attainable in atmospheric flows. Our results point to a Reynolds number-independent logarithmic correction to the classical power law for decaying turbulence that calls for theoretical understanding.

DOI: [10.1103/PhysRevLett.131.024001](https://doi.org/10.1103/PhysRevLett.131.024001)

Introduction.—Turbulent flows feature a self-organized net transfer of kinetic energy from the large energetic length scales (L) to the small viscous and dissipative scales (η). The statistical properties of incompressible turbulent flows in the inertial range ($\eta \ll r \ll L$) have long been proposed to depend only on the rate of kinetic energy transfer (ϵ) and otherwise to follow universal relations [1]. Universality, thus, is expected to emerge as the turbulence intensity, i.e., the Reynolds number increases—the larger it is, the larger the expected universal inertial range should be. This prediction relies on dimensional arguments and is supported to some extent by experiments and by numerical simulations of the Navier-Stokes equation [2–5]. The central parameter is the Reynolds number given by

$$R_\lambda \equiv \frac{u' \lambda}{\nu} \quad (1)$$

(also known as the Taylor-scale Reynolds number), where u' is the rms velocity of the velocity fluctuations, $\lambda^2 = 15\nu u'^2/\epsilon$ is the (square of the) Taylor scale, and ν is the kinematic viscosity.

In his seminal work, called K41, Kolmogorov [1] assumed that the statistics of a given flow are defined entirely by the rate of energy transfer to dissipation ϵ in the inertial range. Dimensional analysis then leads to the inertial-range scaling law

$$S_n(r) = C_n(\epsilon r)^{n/3}, \quad (2)$$

where the structure function of n th order is given by $S_n(r) = \langle [(\mathbf{u}(\mathbf{x}) - \mathbf{u}(\mathbf{x} + \mathbf{r})) \cdot \mathbf{r}/|\mathbf{r}|]^n \rangle$. It is well known that the intermittent spatial distribution of ϵ leads to a dependence of the inertial-range scaling exponent of the longitudinal structure function S_n on n that is a convex function of n and different from $n/3$ [6]. This does not hold

Published by the American Physical Society under the terms of the [Creative Commons Attribution 4.0 International](https://creativecommons.org/licenses/by/4.0/) license. Further distribution of this work must maintain attribution to the author(s) and the published article's title, journal citation, and DOI. Open access publication funded by the Max Planck Society.

for $n = 3$, where the inertial-range scaling exponent is unchanged by the presence of intermittency.

Scaling is expected to hold in the limit $R_\lambda \rightarrow \infty$ for statistically homogeneous and isotropic turbulence and there will always be corrections to these power laws in real flows and noninfinite Reynolds numbers. However, these corrections are expected to diminish with an increasingly extended inertial range, i.e., with increasing R_λ . One way for power laws to be approached, for example, would be for the local slope of the structure functions to become constant and independent of r within an interval of spatial scales that increases with Reynolds number.

The way in which the limit of large R_λ is approached appears to depend on the type of flow. For instance, it has been observed that structure functions in numerical simulations in a periodic box forced continuously at large scales may approach power laws faster with increasing R_λ than in grid-generated turbulence decaying in wind tunnels (e.g., [7–9]). Atmospheric flows exhibit the largest R_λ and the largest scale separation of any available data, but also exhibit anisotropy and nonstationarity that tend to obscure scaling [3,10–12]. Low temperature liquid helium laboratory flows (e.g., [13]) reach atmospheric Reynolds numbers, but have until now been constrained by a lack of instrumentation with sufficient resolution [14–16].

In this Letter, we present experimental results from decaying turbulent flows in the Max Planck Variable Density Turbulence Tunnel over a wider range of R_λ than in any previous experiment and find that $\zeta_2(r)$ —a measure for the local scaling exponent observed at a given r , see Eq. (3)—is independent of the Reynolds number, but dependent on the separation r . We discuss the possible physical origins of this unexpected result and consequences of the finding.

Experiment and results.—In the Max Planck Variable Density Turbulence Tunnel (VDTT) 88 m³ of sulphur hexafluoride (SF₆) at pressures between 1 and 15 bar are circulated at up to 5.5 m/s. Turbulence is generated with an active grid with individually controllable paddles [17,18] at the inlet of a measurement section. The turbulence in the main measurement location on the tunnel center line 8.3 m downstream from the active grid is approximately statistically homogeneous and isotropic [18,19]. The developing turbulent boundary layers on the tunnel walls do not influence the central measurement region, and the turbulence decays downstream from the grid [20,21].

In the VDTT, the Reynolds number can be adjusted in three different ways by changing (i) the kinematic viscosity ν with pressure, (ii) the energy injection scale L with the active grid protocol, and (iii) the fluctuation velocity u' with the mean flow speed. The primary means, however, of effecting large changes in the Reynolds number was by the first mechanism (i), so that the small scales [$\eta = (\nu^3/\varepsilon)^{1/4}$] differed by up to 2 orders of magnitude between experiments, while the large scales differed by up to a factor of 4.

We recorded time series of the streamwise velocity using MEMS-fabricated 30 μm hot wires (nanoscale thermal anemometry probes, NSTAPs) [22–24] and conventional hot wires. The time series were converted into one-dimensional spatial velocity fields by assuming the advection of turbulent fluctuations with the local mean velocity U , i.e., $x = Ut$ (Taylor’s hypothesis) [25]. We have verified that the turbulence intensities found in our experiments allow the application of Taylor’s hypothesis by studying the effect of a random sweeping model [26,27] on model spectra [21,28] and by comparing the results of experiments with different turbulence intensities. In all experiments, the wire lengths were $\lesssim 4\eta$. Details on the active grid as well as the measurement accuracy can be found in the Supplemental Material [29], which includes Refs. [17,22,24,30–36].

Here we investigate structure functions (S_n) and their slopes as functions of the scale r/η (Fig. 1). These functions can typically be separated into three regimes: the viscous subrange [where S_2 approaches $(r/\eta)^2$ toward small scales], the inertial subrange [where it is hypothesized that $S_2 \sim (r/\eta)^{\zeta_2}$], and the large scales (where S_2 approaches $2u'^2 = \text{const}$ toward large scales). Figure 1 (upper) shows S_2 and S_3 compensated by the K41 predictions [Eq. (2)], so that the inertial subrange presents as an approximate plateau, one that extends to larger r/η at larger R_λ . We compare with atmospheric measurements (at $R_\lambda \approx 17\,000$ [10]) and recent computer simulation of the Navier-Stokes equations in a periodic box (at $R_\lambda = 2250$ [5]). The data have been collapsed artificially at $r/\eta = 10$ to offset errors in measurements of ε . The direct numerical simulation (DNS) data are in approximate agreement with our data up to about $10^3\eta$, where the experimental curves fall beneath the DNS. This difference occurs at scales that we show below are R_λ -independent in the experiment. The difference between the experiments and DNS may be attributed to the forcing scheme applied in computer simulations at large scales [37].

We take special note of the third-order structure function at $R_\lambda = 2680$, since an exact result exists for the S_3 (and not for any other order) at $R_\lambda \rightarrow \infty$, which is the 4/5 law, $S_3 = -(4/5)\varepsilon r$ [1,38]. Figure 1(top) shows that the data approach this scaling approximately in the vicinity of 200η .

To reveal power laws unambiguously, it is convenient to study the slopes of the structure functions or the local scaling exponents as functions of r ,

$$\zeta_n(r) \equiv \frac{d \log(S_n)}{d \log(r)}, \quad (3)$$

where $\zeta_n(r)$ is a constant independent of r wherever scaling laws prevail. We observe in Fig. 1 (bottom) that $\zeta_2(r)$ decreases monotonically. As expected due to intermittency, we do not observe the K41 prediction of $\zeta_2 = 2/3$. Models of intermittent turbulence predict $\zeta_2 \gtrsim 2/3$ (e.g., [6]), consistent with a region of approximately constant $\zeta_2 \approx 0.73$ that we find between 100η and 200η .

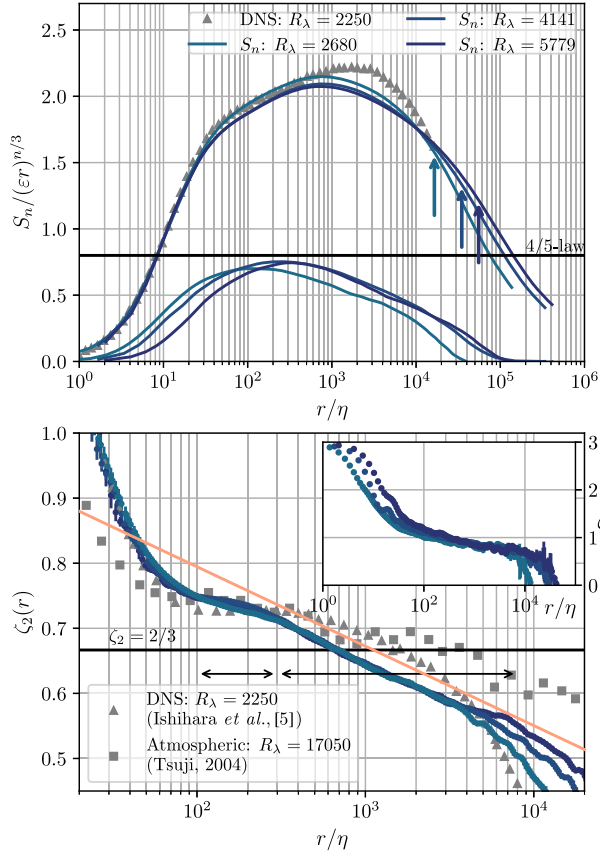


FIG. 1. Top: S_2 and S_3 (S_3 trusted for $r > 50\eta$) compensated by the K41 predictions at three Reynolds numbers and compared with numerical simulations at $R_\lambda = 2250$ [5] (gray triangles). The arrows indicate $r = L$. S_3 approaches the 4/5 law between about 150η and 300η , and the tilt of $S_2/(\epsilon r)^{2/3}$ toward a positive slope in this interval is a signature of intermittency, which generates $\zeta_2 > 2/3$. Bottom: the local slopes $\zeta_2(r)$ [Eq. (3)] reveal additional details in the shapes of the structure functions, including a monotonic decrease over a range of scales up to and beyond $L \gtrsim 10^4\eta$. In addition to $\zeta_2(r)$ of the datasets above, we show atmospheric data at $R_\lambda \approx 17000$ [10] (gray squares). The orange line is for reference and is proportional to $1 - b \log(r/\eta)$. The black arrows indicate the subranges we identify within the inertial range. Inset: local slope of S_3 for the three VDTT datasets.

In any case, $L \gtrsim 10^4\eta$ for these data, so that scaling would be expected between $\eta < r < 10^4\eta$ and far beyond 200η . In contrast to this expectation, note that in the interval of scales between about 300η and 5000η , ζ_2 is not constant and depends on r , decreasing from above 0.7 to below 0.6 (and below $2/3$ given by K41). Within this range, it appears that $\zeta_2(r)$, whatever its shape, is independent of R_λ .

To further interrogate the evolution of the structure functions with increases in the Reynolds number, we compare the local slopes [Eq. (3)] measured at different Reynolds numbers. Figure 2 shows the differences (β_2) between the local slopes measured at the highest R_λ (5779) and those measured at lower R_λ , such that

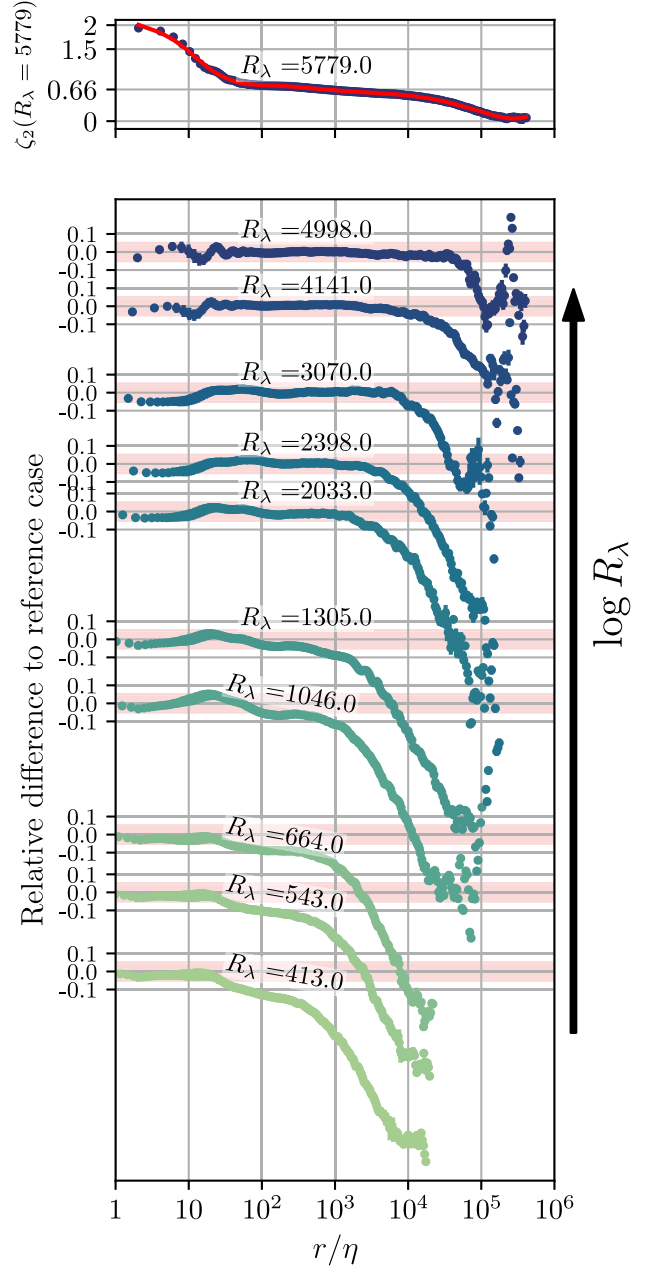


FIG. 2. Bottom: the local scaling exponent differences $\beta_2(r, R_\lambda)$ [Eq. (4)] from their values at $R_\lambda = 5779$ for $413 \leq R_\lambda \leq 4998$. The local slopes for $R_\lambda = 5779$ are reproduced from Fig. 1. Red shading indicates $\pm 5\%$ intervals. The data have been shifted vertically in proportion to $\log(R_\lambda)$, and the colors indicate $\log(R_\lambda)$. A representative sample of 29 datasets is shown. Top: reference case $\zeta_2(r)$ measured at $R_\lambda = 5779$. The red line indicates the smoothed data used to calculate $\beta(r, R_\lambda)$.

$$\beta_2(r, R_\lambda) = \frac{\zeta_2(r, R_\lambda) - \zeta_2(r, 5779)}{\zeta_2(r, 5779)}. \quad (4)$$

For this calculation, the local slope at the highest R_λ has been smoothed with splines to suppress noise (see red line in Fig. 2, top). At viscous scales $r \lesssim 20\eta$, we find that

$\beta(r, R_\lambda) \approx 0$ for all R_λ , indicating the expected universality of the scaling exponent in the viscous subrange, where $\zeta_2 = 2$. Data for which $R_\lambda \gtrsim 2000$ also exhibit a range of scales where $\beta(r) \approx 0$ at intermediate scales $r \gtrsim 100\eta$, indicating that for these cases the local slopes (ζ_2)—whatever their particular values—are close to those in the highest Reynolds number dataset. For instance, the differences in $\zeta_2(r)$ between $R_\lambda = 2033$ and $R_\lambda = 5779$ are less than $\pm 5\%$ within about one decade in r/η . Above $R_\lambda \approx 3000$ this range further extends to over two decades in r/η . The implication is that, throughout these intermediate scales, $\zeta_2(r)$ does not change with increases in R_λ . That is, while S_2 remains r dependent in a way not described by power laws, S_2 does not appear to depend on R_λ at intermediate scales $10^2 < r/\eta < 10^4$.

In summary, we observe two subranges in structure functions (indicated by the black arrows in the lower panel of Fig. 1) consistent with other laboratory experiments, DNS, and the experiments in the atmosphere: (1) a narrow interval centered near $r \approx 150\eta$, whose width is approximately constant despite increases in R_λ and within which a scaling exponent may be identified that is approximately the same for the experiments, DNS, and atmosphere ($\zeta_2 \approx 0.73$) and (2) an interval $r > 300\eta$ that widens with increasing R_λ as expected for the inertial range, but within which $\zeta_2(r)$ decreases with increasing r in a way independent of R_λ , albeit with subtle differences between the experimental, DNS, and atmospheric data.

Discussion.—We assembled a dataset of active-grid-generated turbulence over a wider range of R_λ than ever before measured in a single setup and found that the second-order velocity increment statistics quantified by $\zeta_2(r)$ is independent of R_λ , but remains dependent on r within a broad range of intermediate scales consistent with the inertial range. The short range of approximately constant ζ_2 near $r/\eta \approx 150$ is consistent with the oscillation in structure described in Refs. [39,40] and is not necessarily indicative of a nascent power law. In other words, the expected r independence of ζ_2 for $R_\lambda \rightarrow \infty$ is not observed in this dataset.

Our results agree with those from computer simulations and atmospheric flows up to $\approx 400\eta$, noting that our Reynolds numbers are higher than in simulations and our experiments are better controlled than the atmosphere. In the following, we discuss how statistical anisotropy and nonstationarity may impact our results.

It is well known that real flows do not exhibit the ideal conditions of isotropy and statistical stationarity under which the theoretical limits are constructed, which can cause deviations from theoretical predictions [3,7,41–43]. Anisotropic contributions can be separated from isotropic ones by expanding S_n in spherical harmonics, provided one has directional information [43,44]. Scales must be considered relative to the scale of the source of anisotropy, which is on the order of the energy injection scale L .

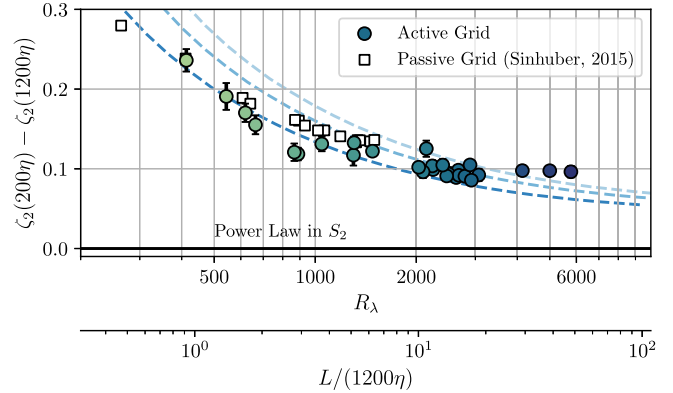


FIG. 3. Difference in the local scaling exponent ζ_2 at two different values of r within the inertial range: 200η , where the statistics can be assumed to be the most isotropic, and 1200η , which tends to be more anisotropic due to its relative proximity to the large scales. When $R_\lambda > 2000$, the inertial range extends from 200η to 1200η and beyond. To the right of this point, changes in the difference of ζ_2 are smaller than to the left. The squares indicate data from the VDTT with a passive grid of rigid bars installed [20]. The light blue lines are a model of decaying turbulence in a confined domain [9] for different choices of the parameter $-A_k$ [0.6 (light), 0.7, 0.9 (dark)]. The black horizontal line indicates power law scaling in S_2 . The measured values of L/η differ slightly from those read off from this graph due to a different ways of estimating $\varepsilon \sim u^3/L$.

Anisotropic contributions decrease relative to isotropic ones toward small scales. We choose $\zeta_2(200\eta)$ as a reference value within the region exhibiting the smallest variation of ζ_2 with respect to changes in r . If anisotropy were the primary contributor to the observed variation in ζ_2 toward larger spatial scales, one would expect that an increase in scale separation $L/\eta \sim R_\lambda^{3/2}$ would tend to cause the anisotropic contributions to diminish. Figure 3 shows that this is not likely the case for $R_\lambda > 2000$: ζ_2 at a fixed scale $r_0 < L$ (we chose 1200η) does not approach $\zeta_2(r = 200\eta)$ with increasing L/η . Thus, anisotropy is unlikely to fully explain the scale dependence of ζ_2 depicted in Fig. 1.

Wind tunnel flows are not statistically stationary due to the downstream decay of turbulent kinetic energy, which is in contrast to computer simulations in periodic boxes that are forced and do not decay. The influence of decay on one-dimensional turbulence statistics can be estimated using closure models for the statistically averaged Navier-Stokes equations (e.g., the Karman-Howarth equation) [38]. We follow Yang *et al.* [9], which accounts for a constant integral length scale, as this condition prevailed approximately in our experiments. We altered the model to include an intermittent inertial-range exponent (see Supplemental Material [29], which includes Refs. [9,45,46]). Adapting the remaining free parameter of the model to fit our data at low R_λ , we estimate that $R_\lambda \approx 10^6$ would be necessary for a decade of inertial-range scaling to appear when the model is applied. These Reynolds numbers are close to those found

on Jupiter [47]. The model, however, does not capture the detailed shape of the observed structure functions. Furthermore, our data suggest an even slower approach (if any) to a power law than the model, which tends to follow the data up to $R_\lambda \approx 2000$, but not beyond (see Fig. 3).

The data do not exclude an R_λ dependence of the odd-order local slopes leading to power-law scaling (including the 4/5 law) at finite R_λ . Our data suggest that $R_\lambda \approx 10^5$ would be required for the 4/5 law to appear. Differences in scaling behavior between odd and even orders have recently been attributed to gradual increases in the velocity time series (ramp) followed by sudden drops (cliff) [48]. In general, third-order statistics are sensitive to the transfer of energy, whereas second-order statistics measure the distribution of energy.

This Letter demonstrates a range of scales outside the viscous range whose shape is R_λ -independent to within experimental error. Our findings suggest that the inertial range is more complex than anticipated and an increase in R_λ might not necessarily yield an approach to power laws. The observed behavior questions the appropriateness of power laws for the description of *real-world* flows at large Reynolds numbers, in general. They therefore ultimately put into question the practical relevance of a separation of turbulence into viscous, inertial, and large scales, at least at a quantitative level.

Max Planck Society provided funding for Open Access Publishing and the VDTT. Volkswagen Foundation provided funding for the VDTT. The operation of the experiment would have been impossible without the help and expertise of A. Kubitzek, A. Kopp, A. Renner, U. Schminke and O. Kurre. The NSTAPs were generously prepared and provided by M. Hultmark and Y. Fan. We thank A. Pumir, M. Wilczek, H. Xu, and D. Lohse for helpful discussions.

*christian.kuechler@ds.mpg.de

†gpb1@cornell.edu

‡eberhard.bodenschatz@ds.mpg.de

- [1] A. N. Kolmogorov, The local structure of turbulence in incompressible viscous fluid for very large Reynolds numbers, *Dokl. Akad. Nauk SSSR* **30**, 301 (1941).
- [2] S. G. Saddoughi and S. V. Veeravalli, Local isotropy in turbulent boundary layers at high Reynolds number, *J. Fluid Mech.* **268**, 333 (1994).
- [3] B. Dhruva, Y. Tsuji, and K. R. Sreenivasan, Transverse structure functions in high-Reynolds-number turbulence, *Phys. Rev. E* **56**, R4928 (1997).
- [4] K. P. Iyer, K. R. Sreenivasan, and P. K. Yeung, Scaling exponents saturate in three-dimensional isotropic turbulence, *Phys. Rev. Fluids* **5**, 054605 (2020).
- [5] T. Ishihara, Y. Kaneda, K. Morishita, M. Yokokawa, and A. Uno, Second-order velocity structure functions in direct numerical simulations of turbulence with R_λ up to 2250, *Phys. Rev. Fluids* **5**, 104608 (2020).

- [6] U. Frisch, *Turbulence: The Legacy of A. N. Kolmogorov* (Cambridge University Press, Cambridge, 1995).
- [7] R. A. Antonia, S. L. Tang, L. Djenidi, and Y. Zhou, Finite Reynolds number effect and the 4/5 law, *Phys. Rev. Fluids* **4**, 084602 (2019).
- [8] D. Fukayama, T. Oyamada, T. Nakano, T. Gotoh, and K. Yamamoto, Longitudinal structure functions in decaying and forced turbulence, *J. Phys. Soc. Jpn.* **69**, 701 (2000).
- [9] P.-F. Yang, A. Pumir, and H. Xu, Generalized self-similar spectrum and the effect of large-scale in decaying homogeneous isotropic turbulence, *New J. Phys.* **20**, 103035 (2018).
- [10] Y. Tsuji, Intermittency effect on energy spectrum in high-Reynolds number turbulence, *Phys. Fluids* **16**, L43 (2004).
- [11] K. R. Sreenivasan and B. Dhruva, Is there scaling in high-Reynolds-number turbulence?, *Prog. Theor. Phys. Suppl.* **130**, 103 (1998).
- [12] H. Kahalerras, Y. Malécot, Y. Gagne, and B. Castaing, Intermittency and Reynolds number, *Phys. Fluids* **10**, 910 (1998).
- [13] B. Rousset, P. Bonnay, P. Diribarne, A. Girard, J. M. Poncet, E. Herbert, J. Salort, C. Baudet, B. Castaing, L. Chevillard, F. Daviaud, B. Dubrulle, Y. Gagne, M. Gibert, B. Hébral, T. Lehner, P.-E. Roche, B. Saint-Michel, and M. Bon Mardion, Superfluid high Reynolds von Kármán experiment, *Rev. Sci. Instrum.* **85**, 103908 (2014).
- [14] B. Saint-Michel, E. Herbert, J. Salort, C. Baudet, M. Bon Mardion, P. Bonnay, M. Bourgoïn, B. Castaing, L. Chevillard, F. Daviaud, P. Diribarne, B. Dubrulle, Y. Gagne, M. Gibert, A. Girard, B. Hébral, T. Lehner, B. Rousset, and SHREK Collaboration, Probing quantum and classical turbulence analogy in von Kármán liquid helium, nitrogen, and water experiments, *Phys. Fluids* **26**, 125109 (2014).
- [15] D. Duri, C. Baudet, P. Charvin, J. Virone, B. Rousset, J.-M. Poncet, and P. Diribarne, Liquid helium inertial jet for comparative study of classical and quantum turbulence, *Rev. Sci. Instrum.* **82**, 115109 (2011).
- [16] J. Salort, É. Rusaouën, L. Robert, R. du Puits, A. Loesch, O. Pirotte, P.-E. Roche, B. Castaing, and F. Chillà, A local sensor for joint temperature and velocity measurements in turbulent flows, *Rev. Sci. Instrum.* **89**, 015005 (2018).
- [17] K. P. Griffin, N. J. Wei, E. Bodenschatz, and G. P. Bewley, Control of long-range correlations in turbulence, *Exp. Fluids* **60**, 55 (2019).
- [18] C. Küchler, G. P. Bewley, and E. Bodenschatz, Experimental study of the bottleneck in fully developed turbulence, *J. Stat. Phys.* **175**, 617 (2019).
- [19] E. Bodenschatz, G. P. Bewley, H. Nobach, M. Sinhuber, and H. Xu, Variable density turbulence tunnel facility, *Rev. Sci. Instrum.* **85**, 093908 (2014).
- [20] M. Sinhuber, E. Bodenschatz, and G. P. Bewley, Decay of Turbulence at High Reynolds Numbers, *Phys. Rev. Lett.* **114**, 034501 (2015).
- [21] C. Küchler, Measurements of turbulence at high Reynolds numbers: From Eulerian statistics towards Lagrangian particle tracking, Ph.D. thesis, Georg August University Göttingen, Göttingen, Germany, 2020, 10.53846/goediss-8490.

- [22] G. Kunkel, C. Arnold, and A. Smits, Development of NSTAP: Nanoscale thermal anemometry probe, in *Proceedings of the 36th AIAA Fluid Dynamics Conference and Exhibit* (American Institute of Aeronautics and Astronautics, San Francisco, California, 2006).
- [23] M. Vallikivi, M. Hultmark, S. C. C. Bailey, and A. J. Smits, Turbulence measurements in pipe flow using a nanoscale thermal anemometry probe, *Exp. Fluids* **51**, 1521 (2011).
- [24] Y. Fan, G. Arwatz, T. W. Van Buren, D. E. Hoffman, and M. Hultmark, Nanoscale sensing devices for turbulence measurements, *Exp. Fluids* **56**, 138 (2015).
- [25] G. I. Taylor, Statistical theory of turbulence, *Proc. R. Soc. A* **151**, 421 (1935).
- [26] M. Wilczek and Y. Narita, Wave-number–frequency spectrum for turbulence from a random sweeping hypothesis with mean flow, *Phys. Rev. E* **86**, 066308 (2012).
- [27] M. Wilczek, H. Xu, and Y. Narita, A note on Taylor’s hypothesis under large-scale flow variation, *Nonlinear Processes Geophys.* **21**, 645 (2014).
- [28] J. Meyers and C. Meneveau, A functional form for the energy spectrum parametrizing bottleneck and intermittency effects, *Phys. Fluids* **20**, 065109 (2008).
- [29] See Supplemental Material at <http://link.aps.org/supplemental/10.1103/PhysRevLett.131.024001> for details on measurement resolution effects, the active grid, and a table of experiments.
- [30] M. Vallikivi and A. J. Smits, Fabrication and characterization of a novel nanoscale thermal anemometry probe, *J. Microelectromech. Syst.* **23**, 899 (2014).
- [31] N. Hutchins, J. P. Monty, M. Hultmark, and A. J. Smits, A direct measure of the frequency response of hot-wire anemometers: Temporal resolution issues in wall-bounded turbulence, *Exp. Fluids* **56**, 18 (2015).
- [32] M. Samie, I. Marusic, N. Hutchins, M. K. Fu, Y. Fan, M. Hultmark, and A. J. Smits, Fully resolved measurements of turbulent boundary layer flows up to $Re_\tau = 20000$, *J. Fluid Mech.* **851**, 391 (2018).
- [33] A. Ashok, S. C. C. Bailey, M. Hultmark, and A. J. Smits, Hot-wire spatial resolution effects in measurements of grid-generated turbulence, *Exp. Fluids* **53**, 1713 (2012).
- [34] H. Sadeghi, P. Lavoie, and A. Pollard, Effects of finite hot-wire spatial resolution on turbulence statistics and velocity spectra in a round turbulent free jet, *Exp. Fluids* **59**, 40 (2018).
- [35] S. C. C. Bailey, G. J. Kunkel, M. Hultmark, M. Vallikivi, J. P. Hill, K. A. Meyer, C. Tsay, C. B. Arnold, and A. J. Smits, Turbulence measurements using a nanoscale thermal anemometry probe, *J. Fluid Mech.* **663**, 160 (2010).
- [36] M. Samie, N. Hutchins, and I. Marusic, Revisiting end conduction effects in constant temperature hot-wire anemometry, *Expt. Fluids* **59** (2018).
- [37] L. Djenidi and R. Antonia, Kármán–Howarth solutions of homogeneous isotropic turbulence, *J. Fluid Mech.* **932**, A30 (2021).
- [38] T. de Karman and L. Howarth, On the statistical theory of isotropic turbulence, *Proc. R. Soc. A* **164**, 192 (1938).
- [39] M. Sinhuber, G. P. Bewley, and E. Bodenschatz, Dissipative Effects on Inertial-Range Statistics at High Reynolds Numbers, *Phys. Rev. Lett.* **119**, 134502 (2017).
- [40] K. P. Iyer, G. P. Bewley, L. Biferale, K. R. Sreenivasan, and P. K. Yeung, Oscillations Modulating Power Law Exponents in Isotropic Turbulence: Comparison of Experiments with Simulations, *Phys. Rev. Lett.* **126**, 254501 (2021).
- [41] R. A. Antonia and P. Burattini, Approach to the 4/5 law in homogeneous isotropic turbulence, *J. Fluid Mech.* **550**, 175 (2006).
- [42] Y. Tsuji, Large-scale anisotropy effect on small-scale statistics over rough wall turbulent boundary layers, *Phys. Fluids* **15**, 3816 (2003).
- [43] L. Biferale and M. Vergassola, Isotropy vs anisotropy in small-scale turbulence, *Phys. Fluids* **13**, 2139 (2001).
- [44] S. Kurien and K. R. Sreenivasan, Anisotropic scaling contributions to high-order structure functions in high-Reynolds-number turbulence, *Phys. Rev. E* **62**, 2206 (2000).
- [45] P. G. Saffman, The large-scale structure of homogeneous turbulence, *J. Fluid Mech.* **27**, 581 (1967).
- [46] Y.-H. Pao, Structure of turbulent velocity and scalar fields at large wavenumbers, *Phys. Fluids* **8**, 1063 (1965).
- [47] R. M. B. Young and P. L. Read, Forward and inverse kinetic energy cascades in Jupiter’s turbulent weather layer, *Nat. Phys.* **13**, 1135 (2017).
- [48] Katepalli R. Sreenivasan, Kartik P. Iyer, and A. Vinodh, Asymmetry of velocity increments in turbulence, *Phys. Rev. Res.* **4**, L042002 (2022).